21.4 A 400μW-RX, 1.6mW-TX Super-Regenerative Transceiver for Wireless Sensor Networks

B. Otis, Y.H. Chee, J. Rabaey

University of California, Berkeley, CA

The emerging field of ad-hoc wireless sensor networks [1] requires small, highly integrated, inexpensive transceivers with very low power consumption (constrained to 1mW average to enable energy scavenging). This transceiver combines a super-regenerative architecture with bulk acoustic wave (BAW) resonators [2] to reduce the power consumption [3], increase the level of integration, and provide selectivity. The principle of super-regeneration achieves a high-RF gain at low bias currents through discrete sampling of the RF input signal with a periodically cycled RF detector oscillator.

A block diagram for the transceiver is shown in Fig. 21.4.1. The OOK transmitter consists of a BAW-referenced oscillator to provide a stable RF carrier and a low-power amplifier (LPA) to provide an efficient power gain. Digital bits are directly modulated onto the carrier by on/off cycling the transmitter. High transmitter efficiency is achieved through direct modulation and careful oscillator/LPA co-design. At the receiving end, the RF input is matched to the 50Ω load presented by the isolation amplifier. This block converts the RF power to a current, injecting it into the detector oscillator while providing isolation between the oscillator and the antenna. The detector oscillator, whose time-varying tank impedance is cycled at 100kHz, samples the RF input signal as an initial condition for its growing exponential, modifying the start-up envelope. Thus, the signal is sampled directly at RF by the detector oscillator, providing a large RF gain (>55dB) for low signal levels. A BAW resonator sets the free-running frequency of the detector oscillator. The envelope of this oscillation is detected by the nonlinear filter, and its 100kHz sampling tone is removed by a pulse width demodulator, leaving a raw OOK analog signal. The baseband signal can be readily detected with an analog matched filter, an A/D with digital baseband, or a 1b slicer with an appropriately placed threshold.

The 1V, 400μA receiver front-end schematic is shown in Fig. 21.4.2. The isolation amplifier comprises an inductively degenerated PMOS LNA with two on-chip inductors. The most power-hungry components in the receiver, the isolation amplifier and detector oscillator, share bias current thereby effectively halving the current consumption of the receiver. The detector oscillator is cycled by the quench signal (V_{quench}), which creates a time varying tank impedance, periodically dissipating the RF energy stored in the BAW resonator through a shunting transistor. The shape of this impedance waveform allows tuning of the receiver gain and bandwidth properties [4]. A square wave (10% duty cycle) impedance waveform allows simple and adaptable quench generation. Because the symbols are oversampled, the exact quench frequency and phase is not crucial, and can be readily supplied from a digital control block. The high-Q nature of the resonant BAW structure, providing a relatively long oscillator time constant and narrow intrinsic bandwidth, reduces the need for precise control over the oscillator transconductance. Fine TX/RX frequency alignment can be achieved with relatively large binary weighted capacitor arrays due to the high-Q resonator. A weak-inversion PMOS nonlinear filtering stage is DC-coupled to the oscillator. This allows the nonlinear bias point shift of the oscillator to add to that of the filter, thereby increasing the signal level to the pulse-width demodulator.

The prototype receiver implementation is shown in Fig. 21.4.7. The active circuit and inductor area is less than 1mm^2. The accompanying 1.9GHz BAW resonator is wirebonded directly to the CMOS die to eliminate board parasitics. The fully integrated matching network, connected directly to the antenna trace, achieves a measured S_{11} of <-10dB at the operating frequency of 1.9GHz and -25dB at 1.7GHz (Fig. 21.4.2). The mismatch in input frequency is corrected in a revised design. The measured eye diagram of the detector oscillator RF signal in the presence of a -80dBm OOK input is shown in Fig. 21.4.3, illustrating the variation in oscillator startup time for "1" and "0" symbols. The measured sensitivity for a BER of 1e-3 is -100.5dBm at 5kbps, displaying negligible degradation over a supply voltage range from 0.9-1.3V. The measured RF small signal bandwidth of the receiver is 0.5 MHz. The measured gain response of the receiver (Fig. 21.4.4) shows the signal-dependent gain characteristic of super-regenerative detectors operated in the saturated oscillator mode. The logarithmic gain response provides the receiver with an inherent automatic gain control (AGC), easing the dynamic range requirements of the baseband circuits.

The transmitter schematic is shown in Fig. 21.4.5. The oscillator employs a BAW resonator to achieve a stable frequency reference with low power consumption. For a given transmit power, a larger oscillator voltage swing allows the LPA to operate with smaller conduction angle and achieve higher efficiency. To maximize the voltage swing, it is desirable to operate at the transition between the current and voltage limited regimes, where further increase in bias current provides diminishing returns in output swing. Hence, co-designing the oscillator and LPA is essential to obtain the optimal transmitter efficiency. The LPA uses a cascode device to improve isolation between the antenna and oscillator, and employs a low loss capacitive transformer to convert the 50Ω antenna to a higher optimal drain impedance for high efficiency operation. Capacitive transformers are preferred over LC matching networks due to the higher Q and smaller area of on-chip capacitors compared to on-chip inductors.

A chip micrograph of the transmitter is shown in Fig. 21.4.7. The oscillator consumes 89μW while providing 140mV output swing. Beyond 200mV, the oscillator enters into the voltage limited regime. The efficiency of the LPA varies only 4.5% over a 200μW to 400μW output power span as shown in Fig 21.4.6. The LPA achieves a maximum efficiency of 27.5% while delivering 380μW. A fully integrated transceiver using these principles has been implemented and is currently in fabrication. The transceiver requires a 1.9mm^2 total die area. It is fully integrated with the exception of 2 BAW resonators and one bondwire inductor for the LPA. The receiver includes an integrated pulse-width demodulator with digitally controllable gain and bandwidth. The transmitter includes a digitally controlled capacitive array to mitigate variability with the bond wire inductance. A digital serial interface controls all transceiver functionality, including front-end biasing, receiver RF frequency, and baseband bandwidth and gain. The complete receiver consumes 450μW and the transmitter delivers 250μW with 25% efficiency.

Acknowledgements:
The authors would like to thank Agilent Technologies and ST Microelectronics for the BAW resonator and CMOS fabrication, respectively. The contributions of Nathan Pletcher and Alan Wei are greatly appreciated. The authors would also like to thank A.M. Niknejad for his valuable suggestions.

References:
[1] J. Rabaey et al., "PicoRadios for Wireless Sensor Networks: The Next Challenge in Ultra-Low Power Design," *ISSCC Dig. Tech. Papers*, pp. 200-201, Feb., 2002.
[2] R. Ruby et al., "Ultra-miniature High-Q Filters and Duplexers Using FBAR Technology," *ISSCC Dig. Tech. Papers*, pp.120-121, Feb., 2001.
[3] B. Otis et al., "An Ultra-Low Power MEMS-Based Two-Channel Transceiver for Wireless Sensor Networks," *Symp. VLSI Circuits*, June, 2004.
[4] A. Vouilloz et al., "A Low-Power CMOS Super-Regenerative Receiver at 1GHz," *IEEE J. Solid State Circuits*, vol. 36, no. 3, pp. 440-451, March 2001.

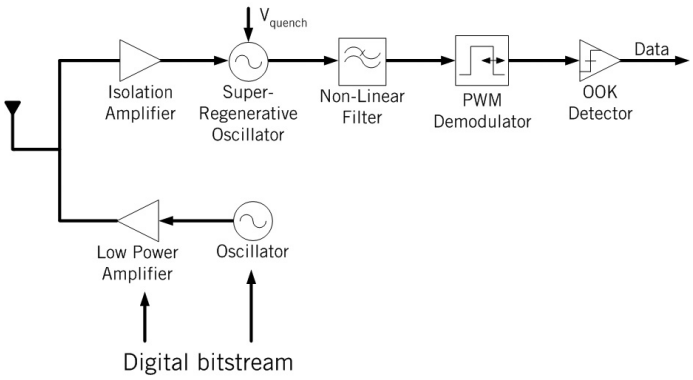

Figure 21.4.1: Transceiver block diagram

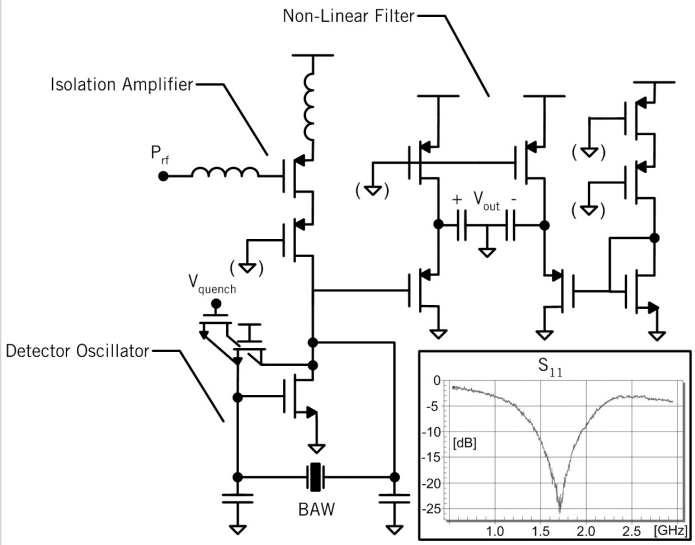

Figure 21.4.2: Receiver front-end schematic and measured input matching.

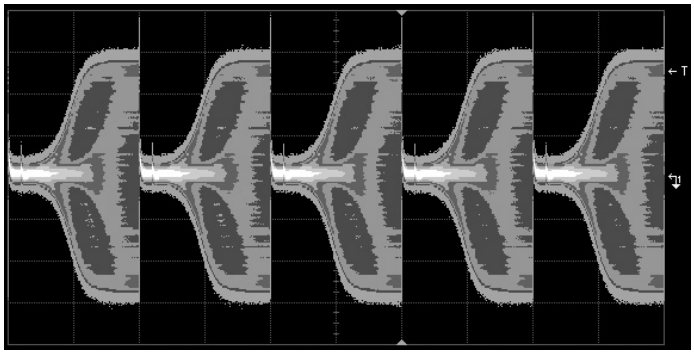

Figure 21.4.3: Detector oscillator eye diagram for -80dBm input.

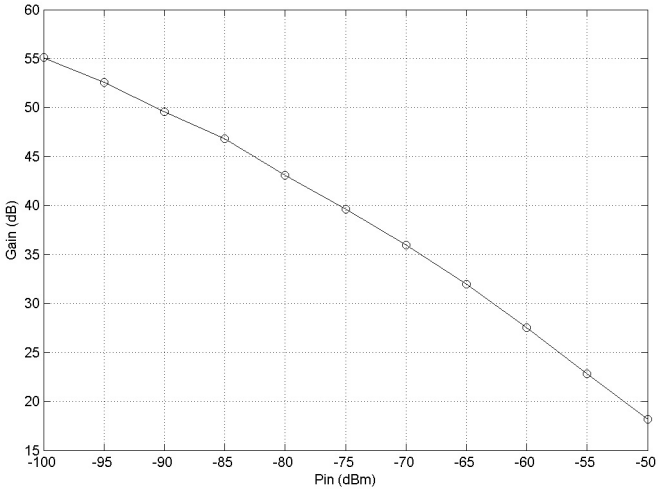

Figure 21.4.4: Logarithmic gain response of the receiver.

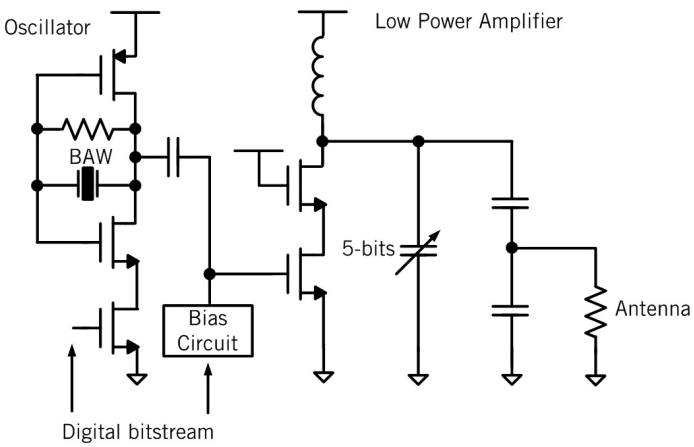

Figure 21.4.5: Transmitter Schematic.

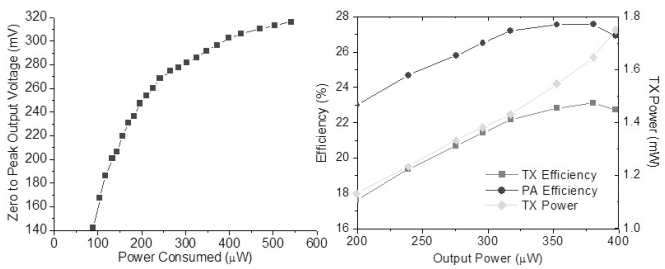

Figure 21.4.6: Oscillator and transmitte performance curves.

Continued on Page 000